Title

THREE-DIMENSIONAL MODELING OF FRACTURES IN ROCK: FROM DATA TO A REGIONALIZED PARENT-DAUGHTER MODEL

Author

Hestir, K.

Publication Date

1987-04-01

Lawrence Berkeley Laboratory
UNIVERSITY OF CALIFORNIA

EARTH SCIENCES DIVISION

Presented at the 1986 AGU Fall Meeting,
San Francisco, CA, December 8–12, 1986

Three-Dimensional Modeling of Fractures in Rock: From Data to a Regionalized Parent-Daughter Model

K. Hestir, J.-P. Chiles, J. Long, and D. Billaux

April 1987

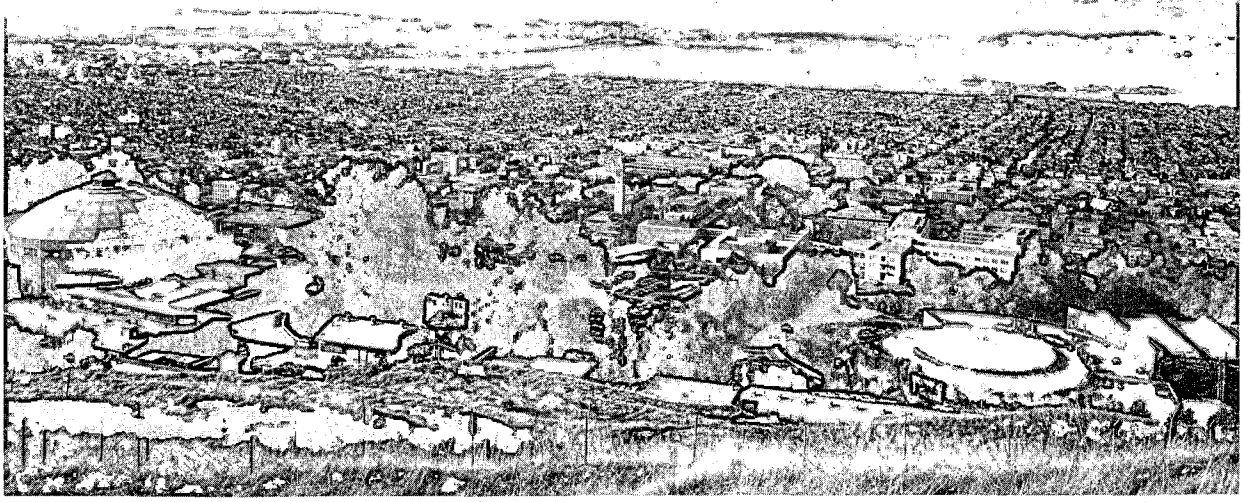

Prepared for the U.S. Department of Energy under Contract DE-AC03-76SF00098

DISCLAIMER

THREE DIMENSIONAL MODELING OF FRACTURES IN ROCK: FROM DATA TO A REGIONALIZED PARENT-DAUGHTER MODEL

Kevin Hestir, Jean-Paul Chiles,[1] Jane Long, and Daniel Billaux[2]

Earth Sciences Division, Lawrence Berkeley Laboratory, University of California, Berkeley, California, 94720

Abstract. We introduce a stochastic model for fracture systems called the parent-daughter model. The model uses circular discs to represent fractures. The discs are placed in three-dimensional space according to a random process called the parent-daughter point process. This process will give a clustering of fractures that cannot be produced with the usual Poisson process. We then outline a procedure for fitting the model to a particular data set.

Introduction

Those who observe fractures in rock often note that the fractures are arranged in swarms or zones. Also, both the density of zones and number of fractures in a zone can vary in space. Our aim is to build a stochastic fracture model which includes these features. Further, we wish to describe a procedure for using field mapping of fractures to identify reasonable parameters for the model.

Stochastic models of fracture networks often employ Poisson processes to generate the fractures [Baecher et al, 1977; Long et al, 1982; Dershowitz, 1985; Robinson, 1985; and others]. A Poisson process model for fractures has the characteristic that placement of each fracture is independent of every other fracture. Thus, there is no spatial correlation between the fractures.

Clearly, if the fractures form swarms and there is a spatial variability of fracture density, there is a spatial correlation between fractures. An appropriate stochastic model for these cases must therefore be more complex than a simple Poisson model. Some work has been done on this problem in two dimensions, [Long and Billaux, 1987] and [LaPointe and Hudson, 1981].

We have developed a three-dimensional model, called the parent-daughter model which includes the features described above. In this model, fractures (daughters) are nucleated around seeds (parents). On a local scale, the parents are randomly located in space. That is, the parents have a Poisson distribution. Over the entire region, however, the density of the parents can vary. The daughter fractures are generated in a cluster around each parent. The number of daughters per parent is a Poisson random variable.

We describe this model in more detail below. We also describe the process for finding the parameters of the model. The fundamental problems in finding parameters are: (1) We have a truncated two-dimensional sample of an extensive three-dimensional system. Large changes in the three-dimensional system produce small changes in the two-dimensional sample; and (2) it is not possible to know where the parents are as there is no "mark" in the rock indicating a parent and it is not always clear to which parent a daughter belongs. Due to these problems we must use trial and error to find the parameters. We choose a reasonable set of parameters by comparing the data which would be derived from the stochastic model to the data derived from the field.

The Parent-Daughter Model

To model fractures we first assume that all fractures are circular discs. We place the discs in space by choosing the locations of their centers according to a random process called a point process. A point process in three-dimensional space is defined as a scheme for randomly placing

[1] On leave from Bureau de Recherches Géologiques et Minières, Orléans, France.
[2] Bureau de Recherches Géologiques et Minières, Orléans, France.

points in space. The most tractable point process to use for the location of disc centers is the Poisson process. This process simply places points in space independently of each other. For this reason the Poisson process will not duplicate the clumping of fractures that is often observed in the field. The doubly stochastic Poisson process and parent-daughter process are generalizations of the basic Poisson process that produce clumps of fractures.

In the following we define the Poisson process, the doubly stochastic Poisson process, and the parent-daughter point process.

A Poisson process with rate λ can be defined by the two properties:

(i) If B is a subset of 3-space with volume V the number of points in B is a Poisson random variable with rate λV, λ a constant.

(ii) The number of points occurring in disjoint volumes of space are independent random variables.

A slight generalization of the Poisson process can be made by replacing the constant rate λ, by a variable rate $\lambda(x,y,z)$. The independence property (ii) is still retained and in property (i) we replace the rate λV with

$$\iiint_B \lambda(x,y,z)dxdydz \quad .$$

To construct a doubly stochastic Poisson process we replace the constant rate λ with random variable rate, $\Lambda(x,y,z)$. Intuitively, we first choose a realization $\lambda(x,y,z)$ of the random function $\Lambda(x,y,z)$, then place points in 3-space according to a Poisson process with rate $\lambda(x,y,z)$. Specifically, a doubly stochastic Poisson process is a point process described by (i) through (iii) below.

(i) $\Lambda(x,y,z)$ is a random variable for each point (x,y,z) in 3-space.

(ii) Given a fixed realization $\lambda(x,y,z)$, of $\Lambda(x,y,z)$, the number of points in B, a subset of 3-space, is a Poisson process with rate

$$\iiint_B \lambda(x,y,z)dxdydz \quad .$$

(iii) Given a fixed realization of $\Lambda(x,y,z)$, the numbers of points in disjoint volumes are independent random variables.

To duplicate the swarming patterns of fractures with a probability model we can place fractures (discs) so that their centers lie on the points of a doubly stochastic Poisson process. These processes give the clumping effect because we see clumps where the rate of the Poisson process is high on the average. The problem with using this model is that the random rate $\Lambda(x,y,z)$ can fluctuate wildly and be quite difficult to estimate. As a result, we have chosen to work with the parent-daughter model which is described below.

The parent-daughter model can be described in the following steps.

- Place points in 3-space according to a doubly stochastic Poisson process. These points will be called parents.
- For each parent pick an independent Poisson number of daughters.
- For each daughter choose an independent displacement from its' parent.
- This yields a series of "daughter points" in 3-space called the parent-daughter point process. Placing discs of random diameter and orientation at each daughter point gives the parent-daughter model for a fracture network.

The advantage of using the parent-daughter point process in comparison to the doubly stochastic Poisson process is that the rate of parents can be taken to be a much smoother random process while swarming effects can be accounted for by other parameters of the model, such as number and location of daughters.

Parameters of the Parent-Daughter Process

The parent-daughter process is completely determined by several parameters. We list these below with a detailed description of the process.

(i) $\Lambda_p(x,y,z)$ will denote the rate of parents. We take Λ_p to be a stationary random function.
(ii) λ_D is the rate of daughters. We take each parent to have an independent Poisson number of daughters with constant rate λ_D.
(iii) $F(x,y,z)$ is the distribution function of the vector displacement from a parent to a daughter. Each daughter is independently placed at a random location from the parent according to the distribution F.
(iv) At each daughter we place a disc so that the center of the disc is at the daughter point. Each disc is independently assigned a diameter according to a lognormal distribution.
(v) Each disc is then given an orientation according to some probability rule.

Specification of each of the quantities (i) through (v) above, completely determines the model.

Data

The data is an extensive drift wall mapping of fracture traces and orientations taken at the uranium mine Fanay-Augéres in Lumison France. An illustration of the trace data appears in Figure 1. A stereo net of fracture orientation is shown in Figure 2. What we see is a two-dimensional slice through a three-dimensional fracture system. Intersections of fractures with the sampling plane appear as traces (line segments) in the sampling plane. The data is a list of the two-dimensional coordinates of trace centers and orientations of most fractures intersecting the sampling plane; there will be some fractures that intersect the sampling plane in such a way that two end points of the intersection do not appear in the sample. Since over 80% of fractures intersect the sampling plane with two endpoints showing, this censoring was not taken into account in the initial fitting of the model. There are techniques for dealing with this censoring error, see, for example, [Massoud, 1987].

Separation of Fractures into Sets

We have divided the fractures into five different sets according to orientation. Figure 2 is a plot of fracture poles and set boundaries. The initial basis for set definition is a classification of fractures according to five different tectonic episodes at Fanay-Augéres but the final set definitions are largely subjective, [Long and Billaux, 1987]. Seven percent, 79 out of 1185, of the fractures do not fall in any set. Figure 3 shows traces of the five different sets in the sampling plane. We fit a different parent-daughter model to each set of fractures.

Orientation Modeling

Orientation is taken to be a stationary random function independent of all other quantities in the model. It might be that aperture or fracture length is related to orientation but we have no evidence of this.

This illustrates one advantage of separating the fractures into sets according to orientation; since we have a different model for each set and fractures within a set have similar orientations, the probability model for orientation is a relatively simple one.

In the following we discuss estimation of the parent-daughter parameters using the sampling plane measurements.

Statistics Taken From Sampling Plane

There are three obvious measurements that can be taken from the sampling plane. They are

- Trace lengths. These can be used to get an estimate of the fracture diameter distribution.
- Trace density. This is the statistic used to check estimates of λ_D, Λ_p, and $F(x,y,z)$.
- Interdistance between traces. This is used to get a heuristic estimate of the dispersion of daughters about parents. A theoretical relationship between the distribution or the variogram of interdistance and the parameters of the parent-daughter model is under development and will greatly aid the fitting of this model.

Diameter Distribution Estimated Using Trace Lengths

Assuming that the diameters of the discs have a lognormal distribution we show how to estimate the parameters of the distribution using the trace lengths. Let

D = diameter of a given fracture.
x = distance between the fracture center and plane of intersection measured parallel to the fracture.
l = the trace length of a fracture in the plane.
$f(D)$ = probability density function of fracture diameters, taken to be lognormal.
$\tilde{f}(D)$ = probability density function of fracture diameters for fractures that intersect a given plane.

$$\overline{D} = \text{mean of } D = \int_0^\infty Df(D)\, dD.$$

Figure 4 illustrates the relationship:

$$l = h(x)$$

$$h^2(x) = D^2 - 4x^2 \quad \text{for } x \leq \frac{D}{2}.$$

$$h^2(x) = 0 \qquad \text{for } x > \frac{D}{2}.$$

The distribution of diameters of fractures intersecting the sampling plane is not the same as the distribution of diameters in space. The reason for this is that a large diameter disc is more likely to intersect the sampling plane than a small diameter disc. Taking this into account, [Warburton, 1980], we get the result

$$\tilde{f}(D) = \frac{1}{\overline{D}} Df(D).$$

Since we assume that the distribution of diameters is lognormal we only need to estimate the first two moments to estimate the distribution. To do this we derive the relationship between the moments of l and the moments of D. First write

$$E(\, l \mid D\,) = \frac{2}{D} \int_0^{\frac{D}{2}} h(x)dx = \frac{\pi D}{4}$$

$$E(\, l^2 \mid D\,) = \frac{2}{D} \int_0^{\frac{D}{2}} h^2(x)dx = \frac{2D^2}{3}.$$

Thus

$$E(\, l\,) = E(\, E(\, l \mid D\,)\,) = \int_0^\infty E(\, l \mid D\,)\tilde{f}(D)dD$$

so

$$E(\,l\,) = \frac{\pi}{4}\frac{E(\,D^2\,)}{E(\,D\,)} \quad .$$

Likewise

$$E(\,l^2\,) = EE(\,l^2 \mid D\,) = \int_0^\infty E(\,l^2 \mid D\,)\tilde{f}(D)dD$$

so

$$E(\,l^2\,) = \frac{2}{3}\frac{E(\,D^3\,)}{E(\,D\,)} \quad .$$

Write

$$\mu_l = \frac{\pi}{4}\frac{E(\,D^2\,)}{E(\,D\,)}$$

$$\mu_l{}^2 + \sigma_l{}^2 = \frac{2}{3}\frac{E(\,D^3\,)}{E(\,D\,)}$$

$$\mu_D = E(\,D\,)$$

and

$$\mu_D^2 + \sigma_D^2 = E(\,D^2\,) \quad .$$

Assuming D has a lognormal distribution we also have

$$\mu_D^3\,(\,1 + \frac{\sigma_D^2}{\mu_D^2}\,)^3 \quad = E(\,D^3\,) \quad .$$

Solving for μ_D and σ_D we get

$$\mu_D = \mu_l \cdot \frac{128}{3\pi^3}\left\{\frac{1}{1 + \dfrac{\sigma_l{}^2}{\mu_l{}^2}}\right\} \tag{1}$$

and

$$\sigma_D = \mu_l \cdot \frac{16}{\pi^2}\left\{\frac{2}{3\,[\,1 + \dfrac{\sigma_l{}^2}{\mu_l{}^2}\,]}\left\{1 - \frac{32}{3\pi^2\,[\,1 + \dfrac{\sigma_l{}^2}{\mu_l{}^2}\,]}\right\}\right\}^{\frac{1}{2}} \quad . \tag{2}$$

We estimate μ_D and σ_D by simply substituting sample values of $\sigma_l{}^2$ and μ_l into (2).

Statistics for Density of Traces

Trace density on the plane sample is our main measurement used for fitting the parent-daughter model to the data. The idea is to measure trace density on sub-areas of the sampling plane, calculate sample covariances between the different sub-areas, then compare these covariances to the theoretical covariances given by the model.

We first introduce some terminology. When we calculate the number or density of traces on a sub-area of the sampling plane we call the sub-area the support of the density. For a stationary random function $\mathbf{X}(t)$ the variogram $\gamma(h)$, of $\mathbf{X}$ is defined by

$$\gamma(h) = \frac{1}{2}\,E(\,(\,\mathbf{X}(t+h) - \mathbf{X}(t)\,)^2\,)$$

$$= \mathrm{var}(\,\mathbf{X}(t)\,) - \mathrm{cov}(\,\mathbf{X}(t+h),\mathbf{X}(t)\,) \quad .$$

Comparison of sample and theoretical covariances is accomplished by comparing sample and theoretical variograms.

Theoretical Variogram for the Parent-Daughter Process

We define some notation. Let

$\mathbf{x}$ be a point in three dimensional space, $\mathbf{R}^3$.
$\Lambda_p(\mathbf{x})$ be the stationary random process for the parent rate.
$\overline{\Lambda}_p$ denote $E(\Lambda_p(\mathbf{x}))$, the average of Λ_p.
$C_{\Lambda_p}(\mathbf{h})$ denotes $E(\Lambda_p(\mathbf{x}+\mathbf{h})\Lambda_p(\mathbf{x}))$, therefore we have $C_{\Lambda_p}(\mathbf{h}) = \mathrm{Cov}(\Lambda_p(\mathbf{x}+\mathbf{h}),\Lambda_p(\mathbf{x})) + \overline{\Lambda}_p^2$.
λ_D be rate of daughters
$F(\mathbf{x})$ be the probability distribution function for the location of a daughter relative to the parent.
B , $\hat{B}$ be supports of density, (ie., sub-areas of the sampling plane).
Q(B) denote the number of traces in B.
$\psi(B,\mathbf{x})$ denotes the probability that a daughter from a parent at $\mathbf{x}$ intersects B.

[Deverly, 1984] has derived an expression for $E(Q(B))$ and $E(Q(B)Q(\hat{B}))$ for a parent-daughter point process. These results have been extended to our model. They show

$$E(Q(B)) = \overline{\Lambda}_p\lambda_D \int_{\mathbf{R}^3} \psi(B,\mathbf{x})\, d\mathbf{x}$$

and

$$\begin{aligned} E(Q(B)Q(\hat{B})) = & \qquad (3)\\ & \lambda_D^2 \int_{\mathbf{R}^3}\int_{\mathbf{R}^3} \psi(B,\mathbf{x})\,\psi(\hat{B},\mathbf{y})C_{\lambda_p}(\mathbf{x}-\mathbf{y})\, d\mathbf{x}\, d\mathbf{y} \\ & + \overline{\Lambda}_p\lambda_D \int_{\mathbf{R}^3} \psi(B\bigcap\hat{B},\mathbf{x})\, d\mathbf{x} \\ & + \overline{\Lambda}_p\lambda_D^2 \int_{\mathbf{R}^3} \psi(B,\mathbf{x})\,\psi(\hat{B},\mathbf{x})\, d\mathbf{x} \quad . \end{aligned}$$

We want to simplify this expression enough to allow easy computer calculation of the theoretical variogram of trace densities. This simplification is given below.

We will use $\mathbf{x} = (x_1,x_2,x_3)$ and $\vec{x} = (x_1,x_2)$ to denote vectors in 3-space and 2-space respectively. Expressions such as $(x_1, x_2, x_3) + (y_1, y_2, y_3)$ will denote the usual vector addition. We write

$$\mathbf{x} = (x_1,x_2,x_3) = (\vec{x},x_3) \quad \text{with} \quad \vec{x} = (x_1,x_2) \quad .$$

For $\vec{x} = (x_1, x_2)$ we also use $B_{-\vec{x}}$ for

$$\{(b_1, b_2) - (x_1, x_2) : (b_1, b_2) \in B\}.$$

Finally, we will use a shorthand for multiple integrals where expressions such as

$$\int f(\vec{x},\vec{y},\vec{z},\vec{w})d\vec{x}\, d\vec{y}\, d\vec{z}d\vec{w}$$

will denote

$$\int_{\vec{x}\in\mathbf{R}^2}\int_{\vec{y}\in\mathbf{R}^2}\int_{\vec{z}\in\mathbf{R}^2}\int_{\vec{w}\in\mathbf{R}^2} f(\vec{x},\vec{y},\vec{z},\vec{w})d\vec{x}\, d\vec{y}\, d\vec{z}\, d\vec{w} \quad .$$

To simplify the formula for the variogram of density we make some additional assumptions about the model.

(i) Discs are perpendicular to the sampling plane and the coordinate system is chosen so that the z-axis is normal to the sampling plane. To compensate for this assumption we must remove an orientation bias from the density measurements. This is discussed in the next section.

(ii) Let $\mathbf{U} = (U_1 , U_2 , U_3) = (\vec{U},U_3)$ be the random displacement of a daughter from a parent. We assume U_1, U_2, U_3 are independent symmetric random variables with densities f_1 , f_2 , f_3 and distributions F_1 , F_2 , F_3. For ease of notation let

$$g(\vec{x}) = g(x_1,x_2) = f_1(x_1)f_2(x_2)$$

and

$$G(\vec{x}) = G(x_1,x_2) = F_1(x_1)F_2(x_2)$$

be the joint density and distribution functions for $\vec{U} = (U_1 , U_2)$.

(iii) Write $\mathbf{h} = (h_1 , h_2 , h_3) = (\vec{h},h_3)$. As we consider only small values of h_3 (up to disc diameters), we can assume

$$C_{\Lambda_p}(\mathbf{h}) = C(\vec{h}) \quad . \tag{4}$$

Let D be a random variable having the distribution of diameters. To simplify notation further we write

$$X_1(B,\vec{x}) = X_1(B,(x_1,x_2)) = P((x_1,x_2) + (u_1,u_2) \in B)$$

and

$$X_2(D,x_3) = P(\frac{-D}{2} < x_3 + U_3 < \frac{D}{2}) \quad .$$

The above assumptions give

$$\psi(B,\mathbf{x}) = P(\vec{x} + \vec{U} \in B)P(\frac{-D}{2} < x_3 + U_3 < \frac{D}{2}) \tag{5}$$

$$= X_1(B,\vec{x})X_2(D,x_3) \quad .$$

Substituting (4) and (5) into (3) and using $B_{\vec{h}} = \hat{B}$, $\mathbf{x} = (x_1,x_2,x_3)$, and $\mathbf{y} = (y_1,y_2,y_3)$, yields

$$E(Q(B)Q(B_{\vec{h}})) \tag{6}$$

$$= \lambda_D^2 \int X_1(B,\vec{x})X_1(B_{\vec{h}},\vec{y})C(\vec{x} - \vec{y})) \, d\vec{x} \, d\vec{y} \tag{6i}$$

$$\times \int X_2(D,x_3)X_2(D,y_3) \, dx_3 \, dy_3 \tag{6ii}$$

$$+ \bar{\Lambda}_p\lambda_D \int X_1(B \cap B_{\vec{h}},\vec{x}) \, d\vec{x} \int X_2(D,x_3) \, dx_3 \tag{6iii}$$

$$+ \bar{\Lambda}_p\lambda_D^2 \int X_1(B,\vec{x})X_1(B_{\vec{h}},\vec{x}) \, d\vec{x} \int X_2^2(D,x_3) \, dx_3 \quad . \tag{6iv}$$

To continue the simplification we give some facts about convolution. Let $w \in S$, $g_1(w)$ and $g_2(w)$ be real valued functions on space S. For our purposes $S = \mathbf{R}^1$ or $S = \mathbf{R}^2$. Let

$$g_1 * g_2(w) = \int_{z \in S} g_1(z)g_2(w - z) \, dz \quad .$$

This is the usual convolution product of g_1 and g_2. If g_1 (or g_2) is an even function (ie., $g_1(-w) = g_1(w)$) then we have the equivalent expression for convolution

$$g_1 * g_2(w) = \int_{z \in S} g_1(z)g_2(w + z) \, dz \quad .$$

Let $B \subseteq S$. The indicator function $I_B(w)$, is defined by $I_B(w) = 1$ if $w \in B$, $I_B(w) = 0$ otherwise. The function $K_B(w)$, called the geometric covariogram of B, is defined by

$$K_B(w) = \int_{z \in S} I_B(w + z)I_B(z) \, dz \quad .$$

Both K_B and g are even functions.

We are now in a position to simplify the terms in (6). Looking at (6i) we can write

$$\int X_1(B,\vec{x})X_1(B_{\vec{h}},\vec{y})C(\vec{x}-\vec{y})\,d\vec{x}\,d\vec{y}$$
$$= \int I_B(\vec{x}+\vec{z})I_B(\vec{w}+\vec{y}-\vec{h})g(\vec{z})g(\vec{w})C(\vec{x}-\vec{y})\,d\vec{z}\,d\vec{w}\,d\vec{x}\,d\vec{y}$$

substituting $\vec{x} = \vec{u} - \vec{z}$ and $\vec{y} = \vec{v} - \vec{w}$ yields

$$\int I_B(\vec{u})I_B(\vec{v}-\vec{h})g(\vec{z})g(\vec{w})C(\vec{u}-\vec{v}+\vec{w}-\vec{z})\,d\vec{z}\,d\vec{w}\,d\vec{u}\,d\vec{v}$$
$$= \int I_B(\vec{u})I_B(\vec{v}-\vec{h})g(\vec{w})g^*C(\vec{u}-\vec{v}+\vec{w})\,d\vec{w}\,d\vec{u}\,d\vec{v}$$
$$= \int I_B(\vec{u})I_B(\vec{v}-\vec{h})g^*g^*C(\vec{u}-\vec{v})\,d\vec{u}\,d\vec{v}\ .$$

Substituting $\vec{v} = \vec{u} - \vec{z}$ gives

$$\int I_B(\vec{u})I_B(\vec{u}-\vec{z}-\vec{h})g^*g^*C(\vec{z})\,d\vec{u}\,d\vec{z}$$
$$= \int K_B(\vec{z}+\vec{h})g^*g^*C(\vec{z})\,d\vec{z} = K_B{}^*g^*g^*C(\vec{h})\ .$$

Next we look at (6ii). If D is fixed then

$$\int X_2(D,x_3)dx_3 = \int I_{(\frac{-D}{2},\frac{D}{2})}(w + x_{3)f_3}(w)dw\,dx_3$$
$$= \int I_{(\frac{-D}{2},\frac{D}{2})}(w + x_{3)f(w)}dx_3dw = D\int f(w)\,dw = D\ .$$

For D random and independent of U_3 we get

$$\int X_2(D,x_3)\,dx_3 = E(D) = \overline{D}\ .$$

So (6ii) equals $\overline{D}^2$. Note that the same argument gives

$$E(Q(B)) = \overline{\Lambda}_p\lambda_D\int \psi(B,\mathbf{x})d\mathbf{x} = \overline{\Lambda}_p\lambda_D\overline{D}(\text{ area B})\ .$$

For (6iii) we have

$$\int X_1(B\cap B_{\vec{h}},\vec{x})\,d\vec{x}$$
$$= \int I_B(\vec{x}+\vec{z})I_B(\vec{x}+\vec{z}-\vec{h})g(\vec{z})\,d\vec{z}\,d\vec{x}\ .$$

Substituting $\vec{x} = \vec{u} - \vec{z}$ yields

$$\int I_B(\vec{u})I_B(\vec{u}-\vec{h})g(\vec{z})\,d\vec{u}\,d\vec{z}$$
$$= K_B(\vec{h})\ .$$
$$= K_B{}^*\delta(\vec{h})$$

where $\delta(\vec{h})$ denotes the Dirac delta functional. So (6iii) equals

$$\overline{\Lambda}_p\lambda_D K_B{}^*\delta(\vec{h})\overline{D}\ .$$

Finally we consider (6iv).

$$\int X_1(B,\vec{x})X_1(B_{\vec{h}},\vec{x})\,d\vec{x}$$
$$= \int I_B(\vec{x}+\vec{z})I_B(\vec{x}+\vec{w}+\vec{h})g(\vec{z})g(\vec{w})\,d\vec{z}\,d\vec{w}\,d\vec{x}\ .$$

Substitute $\vec{x} = \vec{u} - \vec{z}$ to get

$$\int I_B(\vec{u})I_B(\vec{u}+\vec{w}-\vec{z}+\vec{h})g(\vec{z})g(\vec{w})\,d\vec{z}\,d\vec{w}\,d\vec{u}$$
$$= \int K_B(\vec{w}-\vec{z}+\vec{h})g(\vec{z})g(\vec{w})\,d\vec{z}\,d\vec{w}$$

$$= \int K_B{*}g(\vec{w} + \vec{h})g(\vec{w})\, d\vec{w} = K_B{*}g{*}g(\vec{h}) \quad .$$

Next we see $X_2^2(D,x_3) \leq X_2(D,x_3)$ so there is a constant α, $0 < \alpha \leq 1$ such that

$$\int X_2^2(D,x_3)\, dx_3 = \alpha \int X_2(D,x_3)\, dx_3 = \alpha \overline{D} \quad .$$

Therefore

$$E(\, Q(B)Q(B_{\vec{h}})\,) \tag{7}$$
$$= K_B{*}[\overline{D}^2\lambda_D^2 g{*}g{*}C + \overline{\Lambda}_p\lambda_D\overline{D}\delta + \overline{\Lambda}_p\lambda_D^2\alpha\overline{D}g{*}g](\vec{h}) \quad .$$

This form is sufficiently simplified to allow computer estimation of the theoretical variogram of trace density.

Correcting for Orientation Bias

To compare theoretical trace density covariances to data trace density covariance we need to correct for orientation bias. Recall that the theory developed was based on the assumption that fracture discs are perpendicular to the sampling plane. When we measure density in the drift we see density of traces for discs that are not perpendicular to the sampling plane. This causes a bias which we call the orientation bias. To compensate for this we use the following development.

Suppose we have a spatial process with fixed rate λ_V,(ie., the number of disc centers in volume V is $\lambda_V V$). Suppose also, that we have a sampling plane B, and that the normal vector to a disc is at angle θ with B. We take $0 \leq \theta \leq 90$.

Let $\hat{f}(\theta)$ be the density of θ and $\hat{g}(d)$ be the density of the disc diameter,D. For $d_{t_k} \in (d_k, d_k + \Delta d)$ and $\theta_{t_k} \in (\theta_k, \theta_k + \Delta\theta)$ the rate, $\lambda(d_k,\theta_k)$, of discs of diameter d_{t_k} and angle θ_{t_k} intersecting B will be

$$\lambda(d_k,\theta_k) = \lambda_V(\text{area B})d_{t_k}\cos\theta_{t_k}\hat{f}(\theta_{t_k})\hat{g}(d_{t_k})\Delta\theta\Delta d \quad .$$

Hence the total rate, λ_{angle}, of intersecting discs of any diameter and any angle is

$$\lambda_{angle} \approx \sum_k \lambda_V(\text{area B})d_{t_k}\cos\theta_{t_k}\hat{f}(\theta_{t_k})\hat{g}(d_{t_k})\Delta\theta\Delta d$$

or in the limit as $\Delta\theta \to 0$ and $\Delta d \to 0$,

$$\lambda_{angle} = \lambda_V(\text{area B})\overline{D}\overline{\cos\theta} \quad .$$

If all discs were perpendicular to B the total rate would be

$$\lambda_{per} = \lambda_V(\text{area B})\overline{D} \quad .$$

Hence

$$\lambda_{per} = \frac{\lambda_{angle}}{\overline{\cos\theta}} \quad .$$

So we count the number of traces, N, in a support and take the average, $\overline{\cos\theta}$, of $\cos\theta$ for all traces in the support, then use

$$\frac{N}{\overline{\cos\theta}}$$

for our bias corrected density count. This result is equivalent to correction factors given in [Terzaghi, 1965].

Computer Estimation of The Trace Density Variogram

One of the authors [Chiles], has written a program called SALVE that calculates the

theoretical variogram of trace density using (7). The parameters that need to be specified to run the program are:

(i) $\overline{\Lambda}_p$

(ii) λ_D

(iii) Distribution of $\mathbf{U}$ is assumed to be multivariate normal with mean zero and variances σ_1^2, σ_2^2, σ_3^2. The variances must be estimated because they cannot be determined directly from the data.

(iv) The average and standard deviation of disc diameter must be specified. As mentioned before, these are estimated from trace lengths.

(v) $\Lambda_p(\mathbf{x})$ is assumed to be either a Gaussian or lognormal stochastic process. If the Gaussian process is used we must truncate any values below zero. This seems reasonable when $\overline{\Lambda}_p$ is large in comparison to C(0). The covariance structure of Λ_p is specified in geostatistical terms as a mixture of two components each of which can be taken to be spherical or cubic models, [Journel and Huijbregts, 1978; pp 116] and [Chiles, 1977; pp 132].

(vi) The support of the density is specified.

Method of Parameter Estimation

To implement the program note that

$$E(\ Q(B)\ ) = \overline{\Lambda}_p \lambda_D \overline{D}(\text{area of B})$$

so the total number of traces on the plane furnishes an estimate of $\overline{\Lambda}_p\lambda_D$. Hence the parameters we can estimate directly are E(D), var(D), $\overline{\Lambda}_p\lambda_D$. The remaining parameters have no concrete estimates. We therefore resort to heuristic guesses and check the guesses using SALVE. To see an example of the comparison between the theoretical and data variograms see Figure 5.

Obviously, there is much room for improvement in this process. Our present direction is to look for other measurements that can provide statistical estimates of the parameters. Interdistance statistics show some promise for this purpose.

Conclusion

We have discussed fitting a probability model to a 3-dimensional fracture network using data collected from a 2-dimensional slice. Our primary method is to compare trace density covariances to theoretical covariances given by our model. Our preliminary experience shows that this method does not provide enough information to determine all of the parameters of the model. It is however, a useful check of parameter estimates once they are made. To get the estimates, development of a theory for interdistance statistics is recommended.

Acknowledgment. This work was supported through U.S. Department of Energy Contract No. DE-AC03-76SF00098.

References

Baecher, G. B., N. S. Lanney, and H. H. Einstein, Statistical descriptions of rock properties and sampling, Proceedings of the 18th U.S. Symposium on Rock Mechanics, American Institute of Mining Engineers, 1977.

Chiles, J. P, Géostatistique des phénomènes non stationaires, thèse, Université de Nancy-I, 1977.

Dershowitz, W. S., Rock joint systems, Ph.D. Dissertation, Massachusetts Insitute of Technology, 1984.

Deverly, F., Echantillonnage et geostatistique, thèse, Ecole Nationale Superieure des Mines de Paris, 1984.

Journel, A. G. and CH. J. Huijbregts, *Mining Geostatistics*, Academic, London, 1978.

LaPointe, P. R. and J. A. Hudson, Characterization and interpretation of rock mass jointing

patterns, Dept. of Metall. and Miner. Eng., Univ. of Wisc., Madison, Wisc., 1981.

Long, J. C. S. and D. M. Billaux, From field data to fracture network modeling - An example incorporating spatial structure, *Water Resources Research*, in press, 1987.

Long, J. C. S., J. S. Remer, C. R. Wilson, and P. A. Witherspoon, Porous media equivalents for networks of discontinuous fractures, *Water Resources Research*, **18**, 645-658, 1982.

Massoud, H., La modelisation de la petite fractureation par les techniques de la géostatistique, thése, Ecole Nationale de Mines de Paris, 1987.

Robinson, P. C., Connectivity, flow and transport in network models of fractured media, Ph. D. Dissertation, Oxford University, 1984.

Terzaghi, R. D, Sources of error in joint surveys, *Geotechnique*, **15**, 287-303, 1965.

Warburton, P. A., A stereological interpretation of joint trace data, *Int. Jour. Rock Mech. Min. Sci. and Geomech. Abstr.*, **17**, 181-190, Pergamon Press Ltd, 1980.

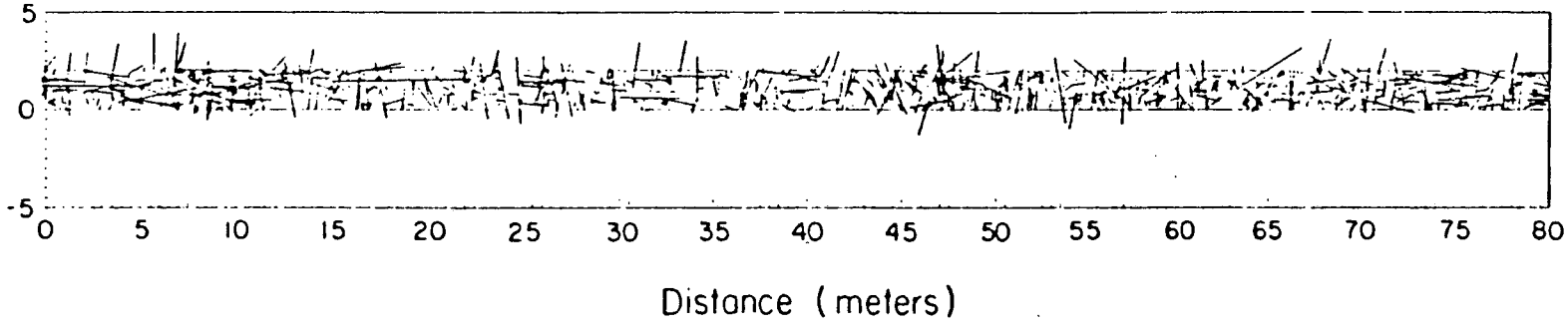

Fig. 1. Plot of fracture traces recorded on an 80 m section of drift wall.

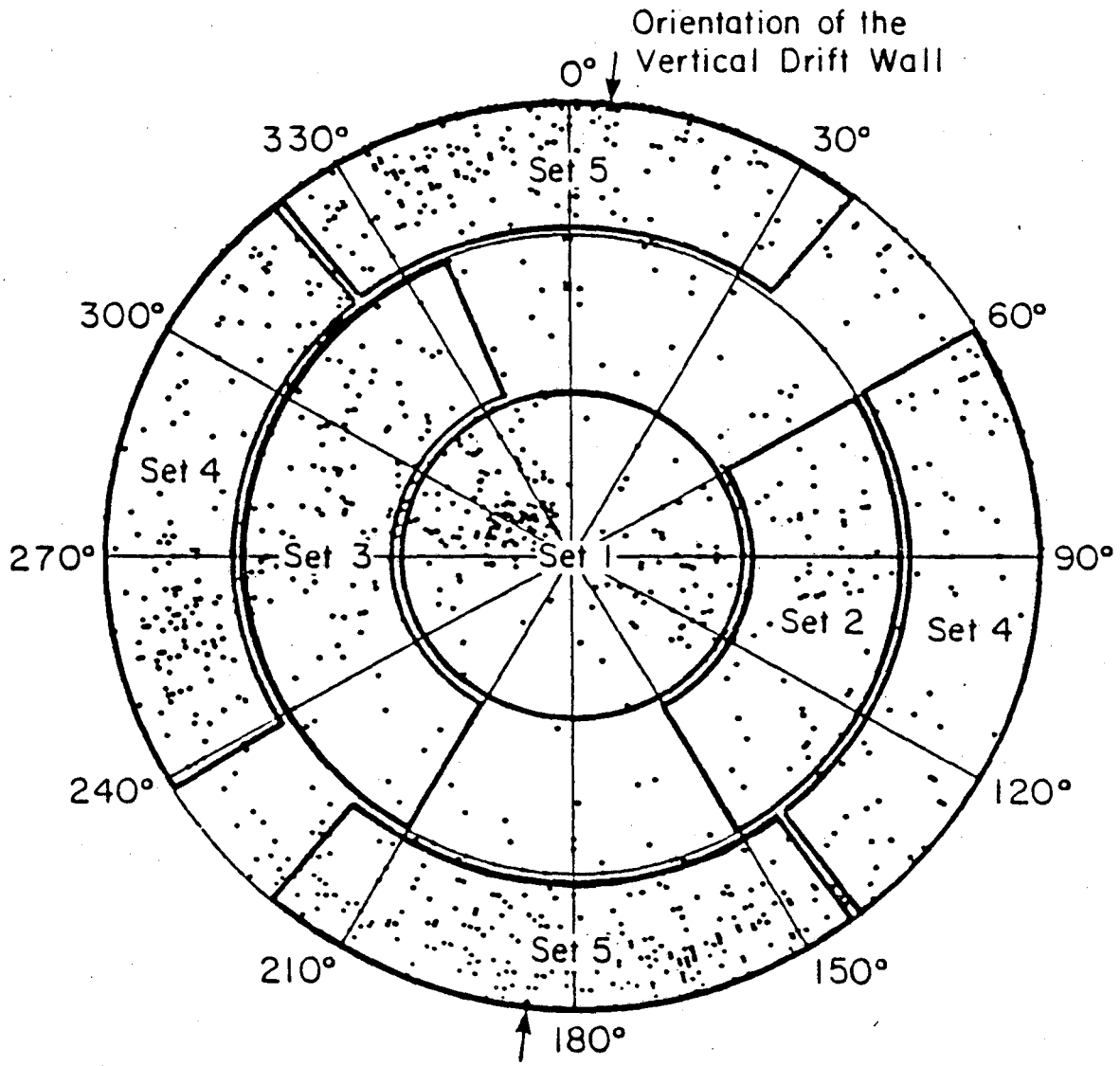

XBL 863-10735

Fig. 2. Stereo net of fracture poles showing set boundaries.

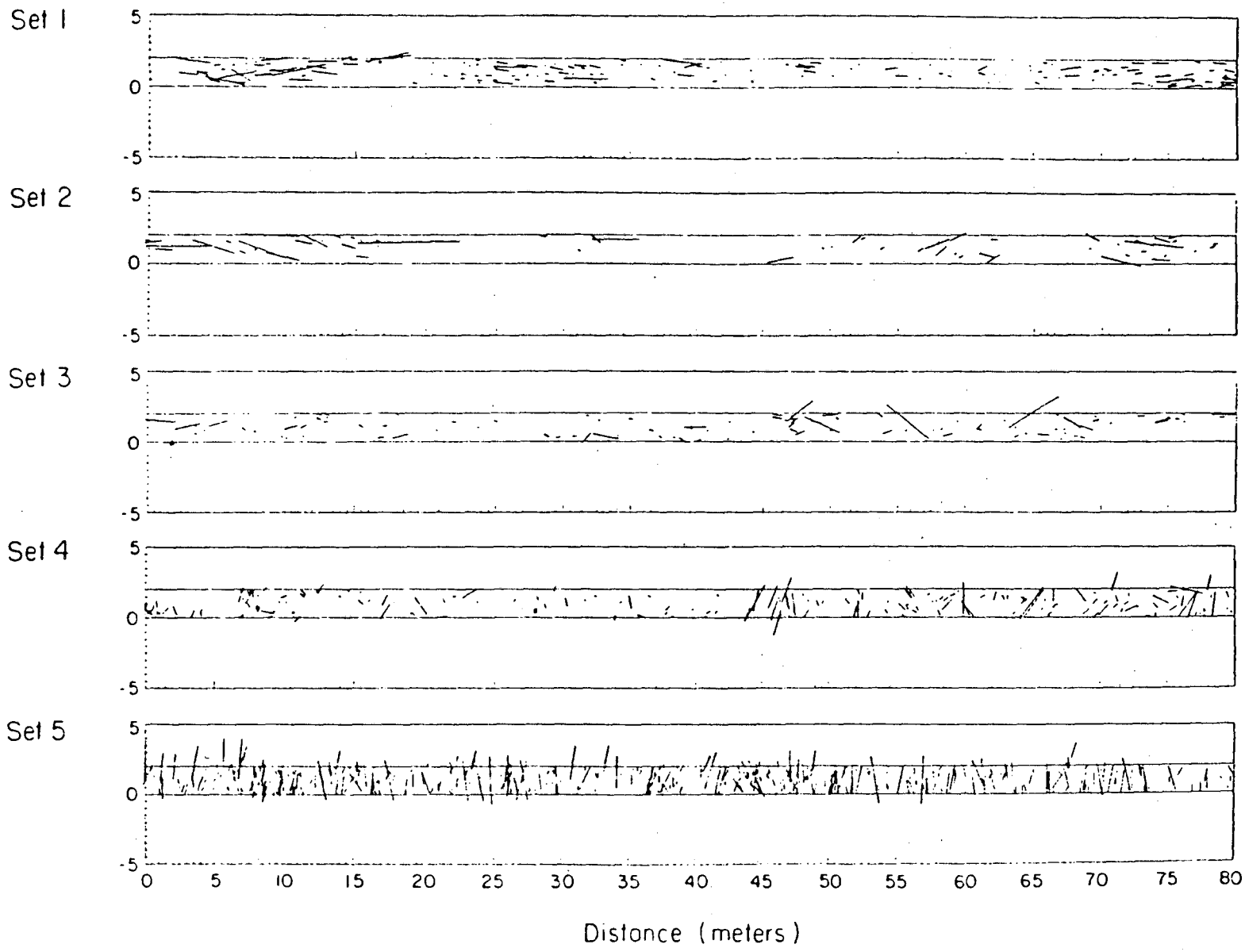

Fig. 3. Plot of recorded fracture traces after division into sets.

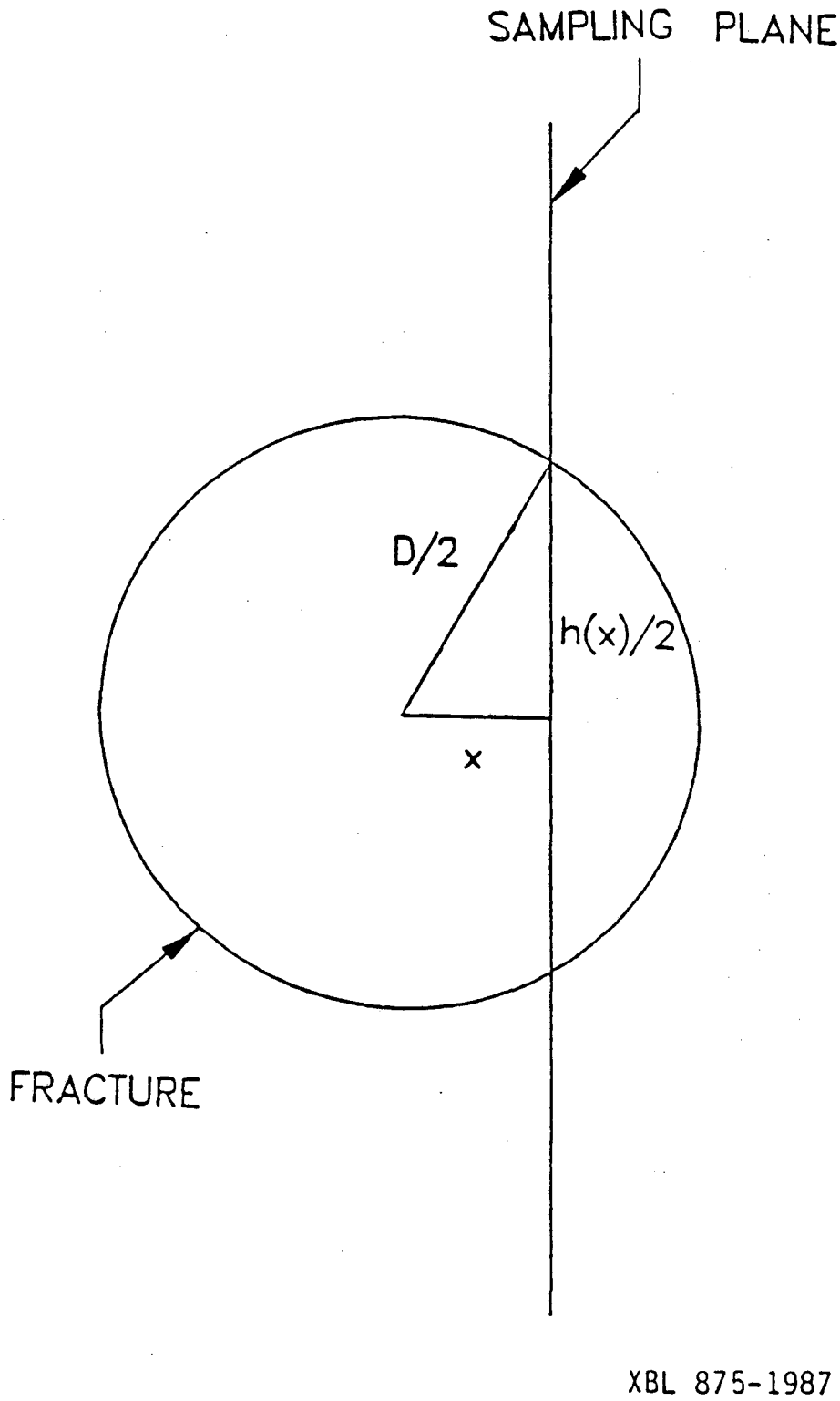

Fig. 4. Fracture disc intersecting sampling plane; diameter of disc = D, trace length = 1.

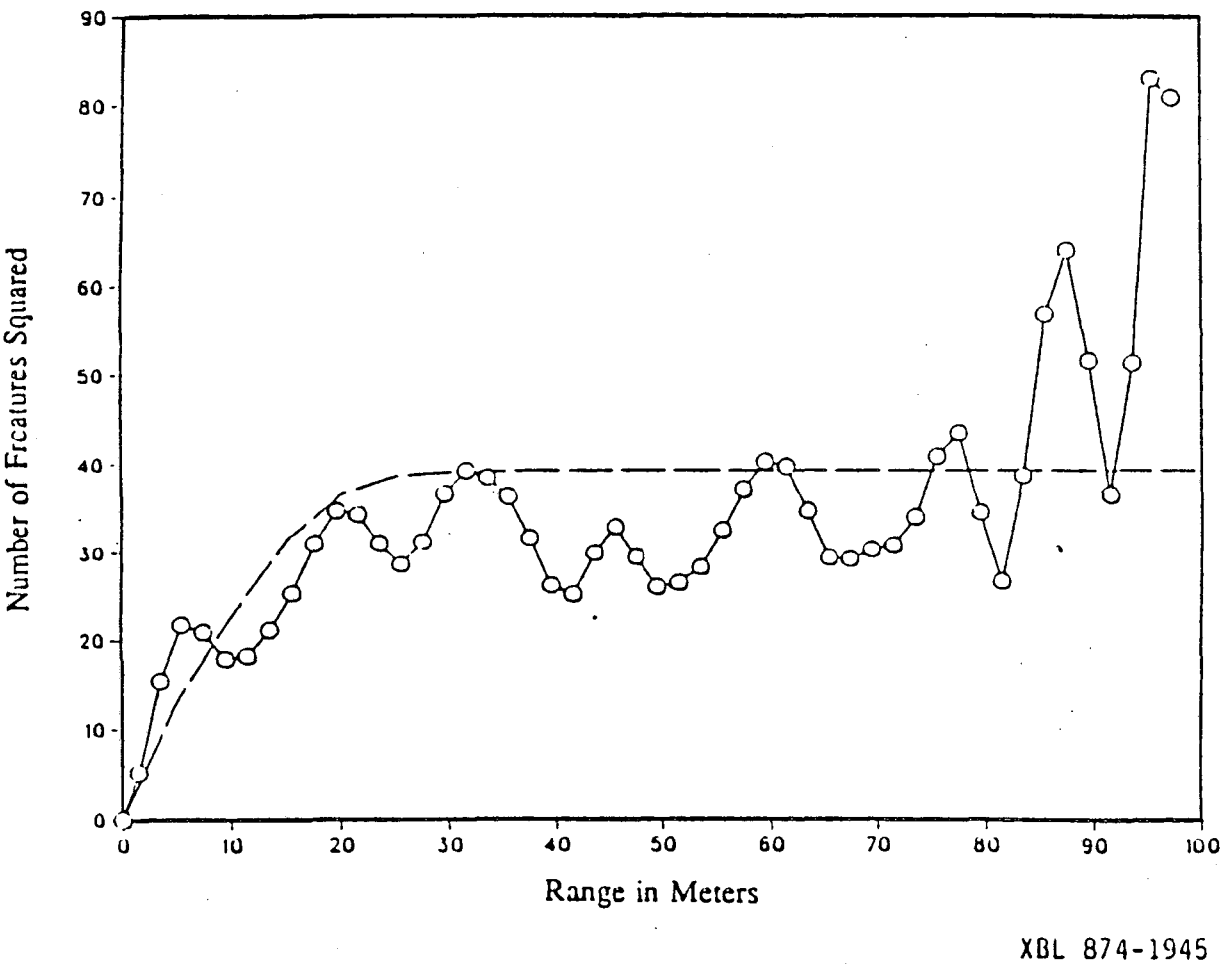

Fig. 5. An example comparison of theoretical and experimental variograms of trace density, O = experimental, –= theoretical, derived from Eq. (7). In this case B is 5m x 2m sub-area of the sampling plane.

LAWRENCE BERKELEY LABORATORY
TECHNICAL INFORMATION DEPARTMENT
UNIVERSITY OF CALIFORNIA
BERKELEY, CALIFORNIA 94720